The Co-existence of Different Synchronization Types in Fractional-order Discrete-time Chaotic Systems with Non–identical Dimensions and Orders

Samir Bendoukha [1] [iD], **Adel Ouannas** [2], **Xiong Wang** [3], **Amina-Aicha Khennaoui** [4], **Viet-Thanh Pham** [5,*], **Giuseppe Grassi** [6] **and Van Van Huynh** [5]

[1] Electrical Engineering Department, College of Engineering at Yanbu, Taibah University, Medina 42353, Saudi Arabia; sbendoukha@taibahu.edu.sa
[2] Department of Mathematics and Computer Science, University of Larbi Tebessi, Tebessa 12002, Algeria; Ouannas@mail.univ-tebessa.dz
[3] Institute for Advanced Study, Shenzhen University, Shenzhen 518060, China; wangxiong8686@szu.edu.cn
[4] Department of Mathematics and Computer Sciences, University of Larbi Ben M'hidi, Oum El Bouaghi 04000, Algeria; kamina_aicha@yahoo.fr
[5] Modeling Evolutionary Algorithms Simulation and Artificial Intelligence, Faculty of Electrical & Electronics Engineering, Ton Duc Thang University, Ho Chi Minh City, Vietnam; huynhvanvan@tdt.edu.vn
[6] Dipartimento Ingegneria Innovazione, Universita del Salento, 73100 Lecce, Italy; giuseppe.grassi@unisalento.it
* Correspondence: phamvietthanh@tdt.edu.vn

Abstract: This paper is concerned with the co-existence of different synchronization types for fractional-order discrete-time chaotic systems with different dimensions. In particular, we show that through appropriate nonlinear control, projective synchronization (PS), full state hybrid projective synchronization (FSHPS), and generalized synchronization (GS) can be achieved simultaneously. A second nonlinear control scheme is developed whereby inverse full state hybrid projective synchronization (IFSHPS) and inverse generalized synchronization (IGS) are shown to co-exist. Numerical examples are presented to confirm the findings.

Keywords: fractional discrete chaos; entropy; projective synchronization; full state hybrid projective synchronization; generalized synchronization; inverse full state hybrid projective synchronization; inverse generalized synchronization

1. Introduction

Discrete-time chaotic systems have been the center of attention in the fields of control [1,2] and secure communications in the last few years [3–6]. This attention can be attributed to two main characteristics. First, the chaotic nature of the dynamical systems, which seems random-like but is in fact completely determined and can be predicted once the initial conditions are known. For instance, this allows for the generation of pseudo–random sequences in secret or private-key encryption. The second interesting property is their discrete nature, which allows for simple implementation and reduced computational complexity. Among the well known discrete-time chaotic systems proposed throughout the years are the Hénon map [7], the Lozi system [8], the generalized Hénon map [9] and the Baier–Klein system [10].

In recent years, researchers have picked an interest in fractional discrete-time chaotic systems. These involve fractional calculus, where the differences in the system's dynamics are fractional. Numerous studies have been dedicated to establishing a framework for fractional discrete calculus such as [11–14]. A good summary of the subject is given in [15].

In general, chaotic systems became of interest in science and engineering in the early 1990s after synchronization was demonstrated. The earliest studies include [16–19]. Since then, various types of synchronization have been proposed in the literature including projective synchronization (PS) [20], generalized synchronization (GS) [21], full state hybrid projective synchronization (FSHPS) [22], and many more. Some modification have also been made to these synchronization types leading, for instance, to inverse generalized synchronization (IGS) [23] and inverse FSHPS (IFSHPS) [24]. With the emergence of fractional chaotic maps such as the fractional Hénon map [25] and the fractional generalized Hénon map [26], the synchronization of such maps became of interest. Very few studies can be found on the subject including [27–32].

Naturally, curiosity grew as to the possibility of multiple synchronization types being achieved simultaneously for the states of the response system. This phenomenon is commonly referred to as the co-existence of synchronization types. Many studies can be found in the literature proposing linear and nonlinear control laws that give rise to the co-existence phenomenon for continuous-time integer-order systems [33], continuous-time fractional systems [34–38], and discrete-time integer-order systems [39–41]. However, to the best of the authors' knowledge, no such studies have been made for fractional-order discrete-time systems. This has motivated us to examine the phenomenon and develop suitable control laws for various types co-existing.

The next section of this paper describes the model for the drive and response systems and defines the necessary notation and synchronization types. Section 3 presents the control law that guarantees the co-existence of PS, FSHPS, and GS as the control laws that establish the co-existence of IFSHPS and IGS. Section 4 presents numerical examples that confirm the validity of the findings. Finally, Section 6 summarizes the work carried out in this paper.

2. System Model

In order to establish the co-existence of different synchronization types in fractional order discrete-time chaotic systems, we consider the generic n-dimensional drive and response pair of the form

$$\begin{cases} {}^{C}\Delta_a^v x_i\left(t\right) = F_i(X\left(t + \alpha - 1\right)), \\ {}^{C}\Delta_a^v y_i\left(t\right) = G_i(Y\left(t + \beta - 1\right)) + u_i, \end{cases} \quad t \in \mathbb{N}_{a+1-v} \tag{1}$$

where $X\left(t\right) = \left(x_1\left(t\right), ..., x_n\left(t\right)\right)^T$, $Y\left(t\right) = \left(y_1\left(t\right), ..., y_n\left(t\right)\right)^T$ represent the states of the drive and response systems, respectively, F_i, G_i are functions from $\mathbb{R}^n$ to $\mathbb{R}$ for $1 \leq i \leq n$, and $u_i, 1 \leq i \leq n$, denote control parameters to be identified by means of the synchronization strategy.

The notation ${}^{C}\Delta_a^v X\left(t\right)$ denotes the v–Caputo type delta difference of a function $X\left(t\right) : \mathbb{N}_a \to \mathbb{R}$ with $\mathbb{N}_a = \{a, a+1, a+2, ...\}$ [12], which is of the form

$$ {}^{C}\Delta_a^v X\left(t\right) = \Delta_a^{-(n-v)} \Delta^n X\left(t\right) = \frac{1}{\Gamma\left(n-v\right)} \sum_{s=a}^{t-(n-v)} \left(t - \sigma\left(s\right)\right)^{(n-v-1)} \Delta^n X\left(s\right), \tag{2}$$

for $v \notin \mathbb{N}$ is the fractional order, $t \in \mathbb{N}_{a+n-v}$, and $n = [v] + 1$. In (2), the v–th fractional sum of $\Delta_s^n X\left(t\right)$ is defined similar to [11] as

$$ \Delta_a^{-v} X\left(t\right) = \frac{1}{\Gamma\left(v\right)} \sum_{s=a}^{t-v} \left(t - \sigma\left(s\right)\right)^{(v-1)} X\left(s\right), \tag{3}$$

with $v > 0$, $\sigma(s) = s + 1$. The term $t^{(v)}$ denotes the falling function defined in terms of the Gamma function Γ as

$$ t^{(v)} = \frac{\Gamma\left(t+1\right)}{\Gamma\left(t+1-v\right)}. \tag{4}$$

Let us, now, define the types of synchronization with which we are interested in our study. The idea is to show that multiple types of synchronization may exist simultaneously for a pair of fractional-order discrete-time chaotic systems.

Definition 1. *If there exists a controller $U = (u_i)_{1 \leq i \leq n}$ and either constants $\gamma \in \mathbb{R}^*$, a matrix Φ, a map $\phi : \mathbb{R}^n \longrightarrow \mathbb{R}^n$, a matrix Θ, or a map $\varphi : \mathbb{R}^n \longrightarrow \mathbb{R}^n$ such that*

$$\lim_{t \to +\infty} \|Y(t) - \gamma X(t)\| = 0 \quad \implies \quad \text{Pair (1) is projective synchronized (PS).}$$
$$\lim_{t \to +\infty} \|Y(t) - \Phi X(t)\| = 0 \quad \implies \quad \text{Pair (1) is full state hybrid projective synchronized (FSHPS).}$$
$$\lim_{t \to +\infty} \|Y(t) - \phi(Y(t))\| = 0 \quad \implies \quad \text{Pair (1) is generalized synchronized (GS).}$$
$$\lim_{t \to +\infty} \|X(t) - \Theta Y(t)\| = 0 \quad \implies \quad \text{Pair (1) is inverse full state hybrid projective synchronized (IFSHPS).}$$
$$\lim_{t \to +\infty} \|X(t) - \varphi(Y(t))\| = 0 \quad \implies \quad \text{Pair (1) is inverse generalized synchronized (IGS).}$$

Note that in Definition 1 above, γ is a constant used to scale the master state vector. Matrices Φ and Θ represent linear transformation of the master and slave state vectors, respectively, and are usually referred to as scaling matrices. The terms ϕ and φ denote some arbitrary maps from $\mathbb{R}^n$ towards $\mathbb{R}^n$. In general, these are nonlinear maps that represent scaling functions. We are now ready to present the main findings of our study.

3. Results

3.1. Co-existence of PS, FSHPS and GS

Let us consider the 2-dimensional drive system and a 3-dimensional response system given, respectively, by

$$^C\Delta_a^v x_i(t) = f_i(X(t + v - 1)), \quad i = 1, 2, \tag{5}$$

and

$$^C\Delta_a^v y_i(t) = \sum_{j=1}^{3} b_{ij} y_j(t + v - 1) + g_i(Y(t + v - 1)) + u_i, \quad i = 1, 2, 3, \tag{6}$$

where $t \in \mathbb{N}_{a+1-v}$, $0 < v \leq 1$, $f_i : \mathbb{R}^2 \longrightarrow \mathbb{R}, 1 \leq i \leq 2$, $(b_{ij}) \in \mathbb{R}^{3 \times 3}$ is the linear part of the drive system, $g_i : \mathbb{R}^3 \longrightarrow \mathbb{R}, 1 \leq i \leq 3$, are nonlinear functions, and $u_i, i = 1, 2, 3$, are controllers to be designed. Based on Definition 1, we may define the co-existence of PS, FSHPS and GS for the coupled systems (5) and (6) as follows.

Definition 2. *It is said that PS, FSHPS and GS co-exist in the synchronization of the drive system (5) and the response systems (6) if there exist a controller $U = (u_i)_{1 \leq i \leq 3}$, a constant $\gamma \in \mathbb{R}^*$, a constant matrix $\Phi = (\Phi_{ij})_{1 \times 2}$, and nonlinear map $\phi : \mathbb{R}^2 \longrightarrow \mathbb{R}$ such that the synchronization errors*

$$\begin{cases} e_1(t) = y_1(t) - \gamma x_1(t), \\ e_2(t) = y_2(t) - \Phi \times (x_1(t), x_2(t))^T, \\ e_3(t) = y_3(t) - \phi(x_1(t), x_2(t)), \end{cases} \tag{7}$$

all satisfy the asymptotic rule

$$\lim_{t \to +\infty} \|e_i(t)\| = 0 \quad \text{for } i = 1, 2, 3. \tag{8}$$

Remark 1. *From the error system (7), it is obvious that states y_1 and x_1 are projective synchronized, y_2 is full state hybrid projective synchronized with x_1 and x_2, and y_3 is generalized synchronized with x_1 and x_2.*

We also need to state the following theorems, which are necessary for the proofs to come.

Theorem 1 ([42]). *The zero equilibrium of the linear fractional-order discrete-time system*

$$^{C}\Delta_a^v e\,(t) = \mathbf{D}e\,(t+v-1)\,, \tag{9}$$

where $e(t) = (e_1(t),...,e_n(t))^T$, $0 < v \le 1$, $\mathbf{D} \in \mathbb{R}^{n\times n}$ and $\forall t \in \mathbb{N}_{a+1-v}$, is asymptotically stable if

$$\lambda \in \left\{ z \in \mathbb{C}:\ |z| < \left(2\cos\frac{|\arg z|-\pi}{2-v} \right)^v \ and\ |\arg z| > \frac{v\pi}{2} \right\}, \tag{10}$$

for all the eigenvalues λ of $\mathbf{D}$.

Next, we propose control laws that achieve the co-existence rule (7). Let us define the matrix $B = (b_{ij})_{3\times 3}$.

Theorem 2. *PS, FSHPS and GS co-exist for the pair (5)–(6) subject to*

$$\begin{cases} u_1 = \sum_{j=1}^3 (c_{1j}-b_{1j})\,e_j\,(t) - \sum_{j=1}^3 b_{1j}y_j\,(t) - g_1\,(Y\,(t+v-1)) + \gamma f_1\,(X\,(t+v-1))\,, \\ u_2 = \sum_{j=1}^3 (c_{2j}-b_{2j})\,e_j\,(t) - \sum_{j=1}^3 b_{2j}y_j\,(t) - g_2\,(Y\,(t+v-1)) + \Phi_1 f_1\,(X\,(t+v-1)) \\ \quad\ +\Phi_1 f_2\,(X\,(t+v-1))\,, \\ u_3 = \sum_{j=1}^3 (c_{3j}-b_{3j})\,e_j\,(t) - \sum_{j=1}^3 b_{3j}y_j(t) - g_3\,(Y\,(t+v-1)) + {}^C\Delta^\beta \phi\,(x_1\,(t)\,,x_2\,(t))\,, \end{cases} \tag{11}$$

where $C = (c_{ij})_{3\times 3}$ is a constant matrix chosen such that all the eigenvalues λ_i of $B - C$ satisfy

$$-2^v < \lambda_i < 0, \quad i = 1,2,3. \tag{12}$$

Proof. The difference equations corresponding to the error system (7) are given by

$$\begin{cases} {}^C\Delta_a^v e_1\,(t) = {}^C\Delta_a^v y_1\,(t) - \gamma\,{}^C\Delta_a^v x_1\,(t)\,, \\ {}^C\Delta_a^v e_2\,(t) = {}^C\Delta_a^v y_2\,(t) - \Phi\,{}^C\Delta_a^v\,(x_1\,(t)\,,x_2\,(t))^T\,, \\ {}^C\Delta_a^v e_3\,(t) = {}^C\Delta_a^v y_3\,(t) - {}^C\Delta_a^v \phi\,(x_1\,(t)\,,x_2\,(t))\,. \end{cases} \tag{13}$$

Substituting the system nonlinearities yields

$$\begin{cases} {}^C\Delta_a^v e_1\,(t) = \sum_{j=1}^3 b_{1j}y_j\,(t+v-1) + g_1\,(Y\,(t+v-1)) + u_1 - \gamma f_1\,(X\,(t+v-1))\,, \\ {}^C\Delta_a^v e_2\,(t) = \sum_{j=1}^3 b_{2j}y_j\,(t+v-1) + g_2\,(Y\,(t+v-1)) + u_2 - \Phi_1 f_1\,(X\,(t+v-1)) \\ \qquad\qquad -\Phi_1 f_2\,(X\,(t+v-1))\,, \\ {}^C\Delta_a^v e_3\,(t) = \sum_{j=1}^3 b_{3j}y_j\,(t+v-1) + g_3\,(Y\,(t+v-1)) + u_3 - {}^C\Delta_a^v \phi\,(x_1\,(t)\,,x_2\,(t))\,. \end{cases} \tag{14}$$

Substituting the proposed control law (11) in (14) yields

$$\begin{cases} {}^C\Delta_a^v e_1\,(t) = \sum_{j=1}^3 (b_{1j}-c_{1j})\,e_j\,(t+v-1)\,, \\ {}^C\Delta_a^v e_2\,(t) = \sum_{j=1}^3 (b_{2j}-c_{2j})\,e_j\,(t+v-1)\,, \\ {}^C\Delta_a^v e_3\,(t) = \sum_{j=1}^3 (b_{3j}-c_{3j})\,e_j\,(t+v-1)\,. \end{cases} \tag{15}$$

In order to show that the zero solution of (16) is globally asymptotically stable, we use the linearization method as described in Theorem 1. The error system (15) can be written in the compact form

$$^{C}\Delta_a^v e\,(t) = (B - C)\,e\,(t+v-1)\,. \tag{16}$$

where $e\,(t) = (e_1\,(t)\,,e_2\,(t)\,,e_3\,(t))^T$. According to condition (12), it is easy to see that all the eigenvalues of the matrix $B - C$ satisfy $|\arg \lambda_i| = \pi > \frac{v\pi}{2}$ and $|\lambda_i| < \left(2\cos\frac{|\arg \lambda_i|-\pi}{2-v} \right)^v$, for $i = 1,2,3$. It, then, follows immediately from Theorem 1 that the zero solution of (16) is globally asymptotically stable and consequently, systems (5) and (6) are synchronized in 3–dimensions according to Definition 2. □

3.2. Co-existence of IFSHPS and IGS

We, now, would like to achieve similar results for the inverse synchronization types listed in Definition 1. Consider the drive and response pair of the form

$$
\begin{cases}
{}^{C}\Delta_a^v x_i\left(t\right) = \sum_{j=1}^{2} a_{ij} x_j\left(t + v - 1\right) + f_i\left(X\left(t + v - 1\right)\right), & i = 1, 2, \\
{}^{C}\Delta_a^v y_i\left(t\right) = g_i\left(Y\left(t + v - 1\right)\right) + u_i, & i = 1, 2, 3,
\end{cases}
\tag{17}
$$

where $t \in \mathbb{N}_{a+1-v}$, $A = \left(a_{ij}\right) \in \mathbb{R}^{2 \times 2}$ and $f_i : \mathbb{R}^2 \to \mathbb{R}$, $1 \le i \le 2$, are nonlinear functions, and $g_i : \mathbb{R}^3 \to \mathbb{R}$, $1 \le i \le 3$. Based on Definition 1, we can state what is meant by the co-existence of IFSHPS and IGS for (17) as summarized in the following definition.

Definition 3. *IFSHPS and IGS are said to co-exist in the synchronization of the pair (17) if there exist controllers u_i, $i = 1, 2, 3$, a constant matrix $\Theta = \left(\Theta_{ij}\right)_{1 \times 3}$, and a map $\varphi : \mathbb{R}^3 \longrightarrow \mathbb{R}$ such that the synchronization errors*

$$
\begin{cases}
e_1\left(t\right) = x_1\left(t\right) - \Theta \times \left(y_1\left(t\right), y_2\left(t\right), y_3\left(t\right)\right)^T, \\
e_2\left(t\right) = x_2\left(t\right) - \varphi\left(y_1\left(t\right), y_2\left(t\right), y_3\left(t\right)\right),
\end{cases}
\tag{18}
$$

all satisfy the asymptotic rule

$$
\lim_{t \to +\infty} e_i\left(t\right) = 0 \ \text{for} \ i = 1, 2.
\tag{19}
$$

Remark 2. *From the error system (18), it is apparent that x_1 is inverse full state hybrid projective synchronized with $y_1\left(t\right)$, $y_2\left(t\right)$ and $y_3\left(t\right)$, and that $x_2(t)$ is inverse generalized synchronized with $y_1\left(t\right)$, $y_2\left(t\right)$ and $y_3\left(t\right)$.*

Suppose that the function φ can be factorized in the form

$$
\varphi\left(y_1\left(t\right), y_2\left(t\right), y_3\left(t\right)\right) = \sum_{j=1}^{3} \theta_j y_j\left(t\right) + \psi\left(y_1\left(t\right), y_2\left(t\right), y_3\left(t\right)\right),
\tag{20}
$$

where θ_j, $j = 1, 2, 3$, are real numbers and $\psi : \mathbb{R}^3 \to \mathbb{R}$ is a nonlinear function. The error dynamics (18) yield the difference equations

$$
\begin{cases}
{}^{C}\Delta_a^v e_1\left(t\right) = {}^{C}\Delta_a^v x_1\left(t\right) - \Theta_1 \, {}^{C}\Delta_a^v y_1\left(t\right) - \Theta_2 \, {}^{C}\Delta_a^v y_2\left(t\right) \\
\qquad\qquad\quad - \Theta_3 \, {}^{C}\Delta_a^v y_3\left(t\right), \\
{}^{C}\Delta_a^v e_2\left(t\right) = {}^{C}\Delta_a^v x_2\left(t\right) - \theta_1 \, {}^{C}\Delta_a^v y_1\left(t\right) - \theta_2 \, {}^{C}\Delta_a^v y_2\left(t\right) \\
\qquad\qquad\quad - \theta_3 \, {}^{C}\Delta_a^v y_3\left(t\right) - {}^{C}\Delta_a^v \psi\left(y_1\left(t\right), y_2\left(t\right), y_3\left(t\right)\right).
\end{cases}
\tag{21}
$$

To simplify the equations, we can define

$$
R_1 = \sum_{j=1}^{2} a_{1j} x_j\left(t\right) + f_1\left(X\left(t\right)\right) - \sum_{j=1}^{3} \Theta_j g_i\left(Y\left(t\right)\right),
\tag{22}
$$

and

$$
R_2 = \sum_{j=1}^{2} a_{2j} x_j\left(t + v - 1\right) + f_2\left(X\left(t\right)\right) - \sum_{j=1}^{3} \theta_j g_i\left(Y\left(t\right)\right) - {}^{C}\Delta_a^v \psi\left(y_1\left(t\right), y_2\left(t\right), y_3\left(t\right)\right).
\tag{23}
$$

Using (22) and (23), (21) may be written in the reduced form

$$
\begin{cases}
{}^{C}\Delta_a^v e_1\left(t\right) = R_1 - \sum_{j=1}^{3} \Theta_j u_j, \\
{}^{C}\Delta_a^v e_2\left(t\right) = R_2 - \sum_{j=1}^{3} \theta_j u_j,
\end{cases}
\tag{24}
$$

or more compactly as

$$^{C}\Delta_a^v e\,(t) = R - M \times (u_1, u_2)^T - (\Theta_3 u_3, \theta_3 u_3)^T, \tag{25}$$

where $R = (R_1, R_2)^T$ and

$$M = \begin{pmatrix} \Theta_1 & \Theta_2 \\ \theta_1 & \theta_2 \end{pmatrix}. \tag{26}$$

To establish the co-existence of IFSHPS and IGS, we assume that M is invertible and denote its inverse by M^{-1}. The control law is, then, given by

$$(u_1, u_2)^T = M^{-1} \times [(L - A)\,e\,(t) + R] \text{ and } u_3 = 0, \tag{27}$$

where $L \in \mathbb{R}^{2 \times 2}$ is a control matrix to be determined. Substituting (27) into Equation (25), we get

$$^{C}\Delta_a^v e\,(t) = (A - L)\,e\,(t + v - 1). \tag{28}$$

The following result follows in a similar manner to Theorem 2. The proof has been omitted as it can be inferred directly from that of Theorem 2.

Theorem 3. *If the control matrix L is chosen such that all the eigenvalues of $A - L$ such that $-2^v < \lambda_i < 0$, $i = 1, 2$, then IFSHPS and IGS co-exist for (17) as described in (18) subject to control law (27).*

4. Numerical Examples

We will now put the theoretical results presented in Section 3 to the test. We consider the 2D fractional Hénon map proposed in [25] as the drive system and the 2D fractional-order generalized Hénon map [26] as the response system. The pair is described as

$$\begin{cases} ^{C}\Delta_a^v x_1\,(t) = x_2\,(t + v - 1) - x_1\,(t + v - 1) + 1 - a_1 x_1^2\,(t + v - 1), \\ ^{C}\Delta_a^v x_2\,(t) = b_1 x_1\,(t + v - 1) - x_2\,(t + v - 1), \end{cases} \tag{29}$$

and

$$\begin{cases} ^{C}\Delta_a^v y_1\,(t) = -y_1\,(t + v - 1) - b_2 y_3\,(t + v - 1) + u_1\,(t + v - 1), \\ ^{C}\Delta_a^v y_2\,(t) = b_2 y_3\,(t + v - 1) + y_1\,(t + v - 1) - y_2\,(t + v - 1) + u_2\,(t + v - 1), \\ ^{C}\Delta_a^v y_3\,(t) = 1 + y_2\,(t + v - 1) - a_2 y_3^2\,(t + v - 1) - y_3\,(t + v - 1) + u_3\,(t + v - 1). \end{cases} \tag{30}$$

The linear and nonlinear parts of the drive system (29) and the response system (30) are given by, respectively,

$$A = \begin{pmatrix} -1 & 1 \\ b_1 & -1 \end{pmatrix}, \quad f = \begin{pmatrix} -a_1 x_1^2\,(t) + 1 \\ 0 \end{pmatrix},$$

and

$$B = \begin{pmatrix} -1 & 0 & -b_2 \\ 1 & -1 & b_2 \\ 0 & 1 & -1 \end{pmatrix}, \quad g = \begin{pmatrix} 0 \\ 0 \\ 1 - a_2 y_3^2\,(t) \end{pmatrix}.$$

These two systems were proposed in the literature and shown to exhibit chaotic behaviors. For instance, when $(a_1, b_1) = (1.4, 0.3)$, $(a_2, b_2) = (0.99, 0.2)$, $a = 0$ and $v = 0.984$. Figures 1 and 2 show the chaotic trajectories of the drive system (29) and response system (29), respectively.

Previous research in information theory has established that entropy quantifies the rate of transfer or generation of information in a particular system. In general, Kolmogorov–Sinai (KS) entropy is applied to measure dynamical systems. A direct time–series approximation of the KS entropy was proposed in [43] named ER entropy, which indicates the level of chaos in a particular system.

Because calculating the exact ER entropy experimentally is difficult, an approximate entropy (ApEn) measure was introduced in [44,45]. Approximate entropy has been used to investigate chaotic systems recently [46,47].

In our work, the approximate entropy values of the drive and response systems have been calculated by using the reported scheme in [44,45]. As a brief summary of the approximation scheme, consider N data samples generated by our fractional map $x\,(1)$, $x\,(2)$, ..., $x\,(N)$. The data is arranged in a sequence of vectors with an embedding dimension m of the form

$$X\,(i) = [x\,(i)\,,\,x\,(i+1)\,,\,...,\,x\,(i+m-1)] \text{ with } 1 \leq i \leq N - m + 1. \tag{31}$$

The distance between two distinct vectors $X\,(i)$ and $X\,(j)$ is denoted by $d\,(X\,(i)\,,\,X\,(j))$. We also define a threshold for our entropy calculation similar to [44,45] as

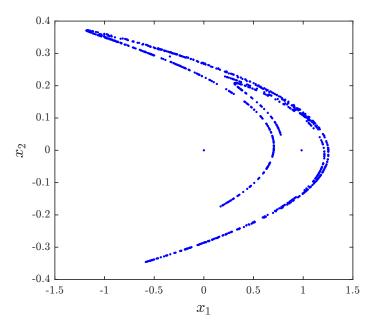$$r = 0.2\text{std}\,(x)\,, \tag{32}$$

with $\text{std}(x)$ being the standard deviation of x. We, then, iterate over the regresser vectors and calculate the number of vectors K that yield a distance $d\,(X\,(i)\,,\,X\,(j)) \leq r$. The approximate entropy is, then, given by

$$\text{ApEn} = \phi^m\,(r) - \phi^{m+1}\,(r)\,, \tag{33}$$

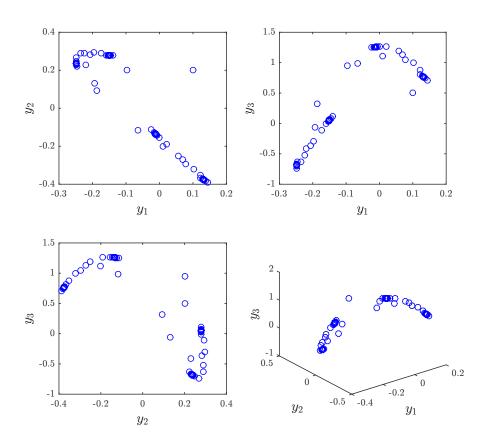where

$$\phi^m\,(r) = \frac{1}{N - m - 1} \sum_{i=1}^{N-m+1} \log\left(\frac{K_i}{N - m + 1}\right). \tag{34}$$

The approximate entropy of the 2D fractional-order Hénon map is ApEn = 0.4159. The approximate entropy of the 2D fractional-order generalized Hénon map is ApEn = 0.0114. The results agree with trajectories illustrated in Figures 1 and 2.

Figure 1. Phase space plot for the fractional Hénon map with $(a_1,\,b_1) = (1.4,\,0.3)$, $v = 0.984$, and $(x_1(0), x_2(0)) = (0,0)$.

Figure 2. Phase portraits for the fractional generalized Hénon map with $(a_2, b_2) = (0.99, 0.2)$, $v = 0.984$, and $(y_1(0), y_2(0), y_3(0)) = (0.1, 0.2, 0.5)$.

Example 1. *The error system for the PS-FSHPS-GS synchronization scheme was described in Definition 2. We let*

$$\gamma = 3, \ \Phi = (1, 3) \ and \ \phi(x_1(t), x_2(t)) = (x_1(t)x_2(t)). \tag{35}$$

Theorem 2 requires the selection of a control matrix C such that all the eigenvalues of $B - C$ satisfy condition (12). For instance, the control matrix C can be chosen as

$$C = \begin{pmatrix} 0 & 0 & 0 \\ 1 & 0 & 0 \\ 0 & 1 & 0 \end{pmatrix}. \tag{36}$$

Simply, we can show that all eigenvalues of $B - C$ are: $\lambda_1 = \lambda_2 = \lambda_3 = -1$ and therefor condition of Theorem 2 is satisfied. We can use the matrix C to construct the following controllers

$$\begin{cases} u_1(t) = & -e_1(t) - b_2 e_3(t) + y_1(t) + b_2 y_3(t) + 3x_2(t) \\ & -3x_1(t) + 3 - 3a_1 x_1^2(t), \\ u_2(t) = & -e_2(t) + b_2 e_3(t) - b_2 y_3(t) - y_1(t) + y_2(t) - 2x_2(t) \\ & + (3b_1 - 1) x_1(t) + 1 - a_1 x_1^2(t) \\ u_3(t) = & -e_3(t) - 1 - y_2(t) + a_2 y_3^2(t) + y_3(t) \\ & + {}^C\Delta_a^v x_1(t) x_2(t). \end{cases} \tag{37}$$

These controllers leads to the simplified error system

$$\begin{cases} {}^{C}\Delta_a^v e_1\,(t) = -e_1\,(t+v-1) - b_2 e_3\,(t+v-1)\,, \\ {}^{C}\Delta_a^v e_2\,(t) = -e_2\,(t+v-1) + b_2 e_3\,(t+v-1)\,, \\ {}^{C}\Delta_a^v e_3\,(t) = -e_3\,(t+v-1)\,. \end{cases} \tag{38}$$

Figure 3 shows the errors as functions of time for parameter sets $(a_1,\,b_1) = (1.4,\,0.3)$ and $(a_2,\,b_2) = (0.99,\,0.2)$, starting point $a = 0$, fractional order $v = 0.984$, and initial errors $(e_1\,(0)\,, e_2\,(0)\,, e_3\,(0)) = (0.1, 0.2, 0.5)$. Clearly, the errors converge towards the zero solution implying that the three slave states are PS–FSHPS–GS synchronized.
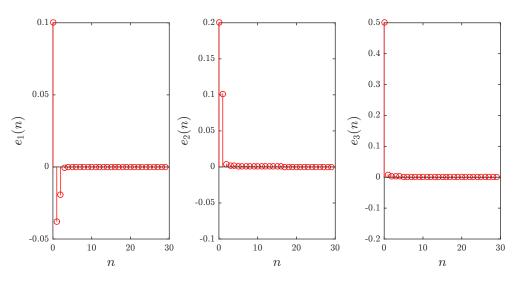

Figure 3. The evolution of errors over time for Example 1.

Example 2. *The second case is concerned with the co-existence of IFSHPS and IGS in 2D. The error system is defined according to Definition 3 where*

$$\Theta = (1, 0, 3) \text{ and } \varphi\,(y_1\,(t)\,, y_2\,(t)\,, y_3\,(t)) = y_1\,(t) + y_2\,(t) + y_3^2\,(t)\,. \tag{39}$$

Following the approach of Theorem 3, we start with a factorization of φ as

$$\varphi\,(y_1\,(t)\,, y_2\,(t)\,, y_3\,(t)) = \sum_{j=1}^{3} \theta_j y_j\,(t) + \psi\,(y_1\,(t)\,, y_2\,(t)\,, y_3\,(t))\,. \tag{40}$$

It can be easily shown that

$$(\theta_1, \theta_2, \theta_3) = (1, 2, 0) \text{ and } \psi\,(y_1\,(t)\,, y_2\,(t)\,, y_3\,(t)) = y_3^2\,(t)\,, \tag{41}$$

are sufficient. The proposed synchronization scheme rearranges Θ and $(\theta_1, \theta_2, \theta_3)$ into the matrix

$$M = \begin{pmatrix} 1 & 0 \\ 1 & 2 \end{pmatrix}, \tag{42}$$

which is invertible with inverse

$$M^{-1} = \begin{pmatrix} 1 & 0 \\ -\frac{1}{2} & \frac{1}{2} \end{pmatrix}. \tag{43}$$

Theorem 3 requires the choice of a matrix L. This may be achieved with

$$L = \begin{pmatrix} 1 & \frac{13}{4} \\ b_1 - 1 & -2 \end{pmatrix}. \tag{44}$$

The controllers can, thus, be constructed according to (27) based on R_1 and R_2 defined in (22) and (23), respectively. We end up with

$$
\begin{cases}
u_1(t) = & -2e_1 - \frac{9}{4}e_2 + x_2(t) - x_1(t) - a_1 x_1^2(t) + y_1(t) \\
& + (b_2 + 3)y_3(t) - 2 - 3y_2(t) + 3a_2 y_3^2(t), \\
u_2(t) = & \frac{3}{2}e_1 + \frac{13}{8}e_2 - y_1(t) + \frac{5}{2}y_2(t) - \left(\frac{3}{2} + b_2\right)y_3(t) \\
& - x_2(t) + \frac{(b_1+1)}{2}x_1(t) + \frac{1}{2}a_1 x_1^2(t) \\
& - \frac{3a_2}{2}y_3^2(t) - \frac{1}{2}{}^C\Delta^\beta y_3^2(t) + 1, \\
u_3(t) = & 0.
\end{cases}
\tag{45}
$$

and

$$
\begin{cases}
{}^C\Delta_a^v e_1(t) = -2e_1(t + v - 1) - \frac{9}{4}e_2(t + v - 1), \\
{}^C\Delta_a^v e_2(t) = e_1(t + v - 1) + e_2(t + v - 1).
\end{cases}
\tag{46}
$$

Figure 4 depicts the stabilized states subject to parameter sets $(a_1, b_1) = (1.4, 0.3)$ and $(a_2, b_2) = (0.99, 0.2)$, starting point $a = 0$, fractional order $v = 0.984$, and initial errors $(e_1(0), e_2(0)) = (-1.6, -0.325)$. It is easy to from Figure 4 that the errors converge towards zero in sufficient time proving that the controllers (45) in fact achieve IFSHPS–IGS synchronization for the pair (29).
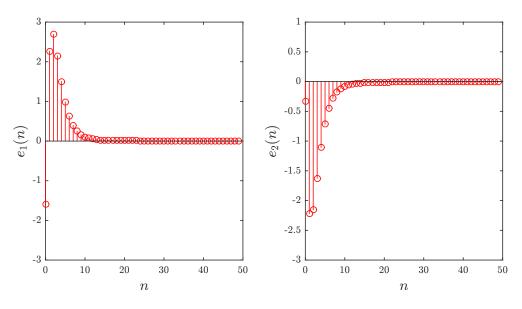

Figure 4. The evolution of errors over time for Example 2.

5. Discussion

In this paper, we have presented novel results concerning the co-existence of multiple synchronization types in Caputo-type fractional chaotic maps. To the best of our knowledge, the topic of co-existence has not been considered before for this type of system, which motivated this research. The synchronization types considered are rather general, which allows for multiple applications, especially in the fields of secure communications and data encryption. In fact, as we mentioned before, very few studies can be found in the literature concerning the synchronization of fractional chaotic maps, which makes this work all the more interesting.

Perhaps the most interesting studies related to the subject are [27–32]. In [27], the authors merely consider a pair of identical fractional logistic maps and propose a simple direct synchronization controller. In [28], an identical synchronization scheme is proposed based on the results of [48,49]. The authors of [29], again, consider the synchronization of identical fractional Hénon maps. The same can be said regarding [32]. As for [31], the authors propose a simple linear feedback controller suitable for a variety of maps. However, it is only shown to achieve complete synchronization, which is the most basic form of synchronization. In [30], the fractional difference operator used is different from the one used here and thus comparison is difficult.

Generally speaking, it is difficult to compare our results to those reported in the above mentioned studies as the scope of our work is much wider. In addition, we are mainly concerned with co-existence, which has not been considered before for this type of systems.

6. Concluding Remarks

In this work, we have shown that different types of synchronization can co-exist for fractional-order discrete-time chaotic systems. We assumed a two dimensional drive system and a three dimensional response system. The main results of the study were two fold. First, we presented a nonlinear control scheme whereby PS, FSHPS, and GS are achieved simultaneously for the three states of the response system. The stability of the zero solution, and consequently the convergence of the synchronization error, was established by means of the stability theory of linear fractional-order discrete-time systems. The second main result concerns the co-existence of IFSHPS and IGS for the same drive-response pair. The three response states are simultaneously IFSHPS synchronized with the first drive state and IGS synchronized with the second drive state. Numerical results have confirmed the findings of the study. Simulations were carried out on Matlab to ensure that the errors converge to zero subject to the proposed control laws.

Author Contributions: Conceptualization, S.B. and A.O.; Formal analysis, X.W. and G.G.; Investigation, S.B.; Methodology, A.O. and V.-T.P.; Software, X.W., A.-A.K. and G.G.; Validation, V.V.H.; Writing – original draft, A.-A.K. and V.-T.P.; Writing – review & editing, V.V.H.

References

1. Kocarev, L.; Szczepanski, J.; Amigo, J.M.; Tomovski, I. Discrete Chaos–I: Theory. *IEEE Trans. Circuits Syst. I Reg. Pap.* **2006**, *53*, 1300–1309. [CrossRef]
2. Li, C.; Song, Y.; Wang, F.; Liang, Z.; Zhu, B. Chaotic path planner of autonomous mobile robots based on the standard map for surveillance missions. *Math. Prob. Eng.* **2015**, *2015*, 263964. [CrossRef]
3. Papadimitriou, S.; Bezerianosa, A.; Bountisb, T.; Pavlides, G. Secure communication protocols with discrete nonlinear chaotic maps. *J. Syst. Archit.* **2001**, *47*, 61–72. [CrossRef]
4. Kwok, H.S.; Tang, W.K.S.; Man, K.F. Online secure chatting system using discrete chaotic map. *Int. J. Bifurc. Chaos* **2004**, *14*, 285. [CrossRef]
5. Banerjee, S.; Kurth, J. Chaos and cryptography: A new dimension in secure communications. *Eur. Phys. J. Spec. Top.* **2014**, *223*, 1441–1445. [CrossRef]
6. Fataf, N.A.A.; Mukherjee, S.; Said, M.R.M.; Rauf, U.F.A.; Hina, A.D.; Banerjee, S. Synchronization between two discrete chaotic systems for secure communications. In Proceedings of the 2016 IEEE Sixth International Conference on Communications and Electronics (ICCE), Ha Long, Vietnam, 27–29 July 2016; pp. 477–481.
7. Hénon, M. A two-dimensional mapping with a strange attractor. *Commun. Math. Phys.* **1976**, *50*, 69–77.
8. Lozi, R. Un atracteur étrange du type attracteur de Hénon. *J. Physique* **1978**, *39*, 9–10.
9. Hitzl, D.L.; Zele, F. An exploration of the Hénon quadratic map. *Phys. D Nonlinear Phenom.* **1985**, *14*, 305–26. [CrossRef]
10. Baier, G.; Sahle, S. Design of hyperchaotic flows. *Phys. Rev. E* **1995**, *51*, 2712–2714. [CrossRef]

11. Atici, F.M.; Eloe, P.W. Discrete fractional calculus with the nabla operator. *Electron. J. Qual. Theory Differ. Equ.* **2009**, *4*, 1–12. [CrossRef]

12. Abdeljawad, T. On Riemann and Caputo fractional differences. *Comput. Math. Appl.* **2011**, *62*, 1602–1611. [CrossRef]

13. Abdeljawad, T.; Baleanu, D.; Jarad, F.; Agarwal, R.P. Fractional sums and differences with binomial coefficients. *Discret. Dyn. Nat. Soc.* **2013**, *2013*, 104173. [CrossRef]

14. Baleanu, D.; Wu, G.; Bai, Y.; Chen, F. Stability analysis of Caputo–Like discrete fractional systems. *Commun. Nonlinear Sci. Numer. Simul.* **2017**, *48*, 520–530. [CrossRef]

15. Goodrich, C.; Peterson, A.C. *Discrete Fractional Calculus*; Springer: Berlin, Germany, 2015.

16. Yamada, T.; Fujisaca, H. Stability theory of synchronized motion in coupled-oscillator. Systems. II: The mapping approach. *Prog. Theor. Phys.* **1983**, *70*, 1240–1248. [CrossRef]

17. Yamada, T.; Fujisaca, H. Stability theory of synchronized motion in coupled-oscillator Systems. III: Mapping model for continuous system. *Prog. Theor. Phys.* **1984**, *72*, 885–894. [CrossRef]

18. Afraimovich, V.S.; Verochev, N.N.; Robinovich, M.I. Stochastic synchronization of oscillations in dissipative systems. *RadioPhys. Quantum Electron.* **1984**, *29*, 795–803. [CrossRef]

19. Pecora, L.M.; Carrol, T.L. Synchronization in chaotic systems. *Phys. Rev. A* **1990**, *64*, 821–824.

20. Grassi, G.; Miller, D.A. Projective synchronization via a linear observer: Application to time-delay, continuous-time and discrete-time systems. *Int. J. Bifurc. Chaos* **2007**, *17*, 1337–1344. [CrossRef]

21. Ouannas, A.; Odibat, Z. Generalized synchronization of different dimensional chaotic dynamical systems in discrete-time. *Nonlinear Dyn.* **2015**, *81*, 765–771. [CrossRef]

22. Ouannas, A. On full state hybrid projective synchronization of general discrete chaotic systems. *J. Nonlinear Dyn.* **2014**, *2014*, 983293. [CrossRef]

23. Ouannas, A. On inverse generalized synchronization of continuous chaotic dynamical systems. *Int. J. Appl. Comp. Math.* **2016**, *2*, 1–11. [CrossRef]

24. Ouannas, A.; Grassi, G. Inverse full state hybrid projective synchronization for chaotic maps with different dimensions. *Chin. Phys. B* **2016**, *25*, 090503. [CrossRef]

25. Hu, T. Discrete Chaos in Fractional Hénon Map. *Appl. Math.* **2014**, *5*, 2243–2248. [CrossRef]

26. Shukla, M.K.; Sharma, B.B. Investigation of chaos in fractional order generalized hyperchaotic Hénon map. *Int. J. Elec. Comm.* **2017**, *78*, 265–273. [CrossRef]

27. Wu, G.; Baleanu, D. Chaos synchronization of the discrete fractional logistic map. *Signal Process.* **2014**, *102*, 96–99. [CrossRef]

28. Wu, G.; Baleanu, D.; Xie, H.; Chen, F. Chaos synchronization of fractional chaotic maps based on the stability condition. *Physica A* **2016**, *460*, 374–383. [CrossRef]

29. Liu, Y. Chaotic synchronization between linearly coupled discrete fractional Hénon maps. *Indian J. Phys.* **2016**, *90*, 313–317. [CrossRef]

30. Megherbi, O.; Hamiche, H.; Djennoune, S.; Bettayeb, M. A new contribution for the impulsive synchronization of fractional-order discrete-time chaotic systems. *Nonlinear Dyn.* **2017**, *90*, 1519–1533. [CrossRef]

31. Xin, B.; Liu, L.; Hou, G.; Ma, Y. Chaos synchronization of nonlinear fractional discrete dynamical systems via linear control. *Entropy* **2017**, *19*, 351. [CrossRef]

32. Khennaoui, A.A.; Ouannas, A.; Bendoukha, S.; Wang, X.; Pham, V.T. On chaos in the fractional-order discrete-time unified system and its control synchronization. *Entropy* **2018**, *20*, 530. [CrossRef]

33. Ouannas, A.; Azar, A.T.; Sundarapandian, A.V. New hybrid synchronization schemes based on coexistence of various types of synchronization between master-slave hyperchaotic systems. *Int. J. Comp. Apps. Tech.* **2017**, *55*, 112–120. [CrossRef]

34. Ouannas, A.; Abdelmalek, S.; Bendoukha, S. Coexistence of some chaos synchronization types in fractional-order differential equations. *Electron. J. Differ. Equ.* **2017**, *2017*, 1–15.

35. Ouannas, A.; Odibat, Z.; Hayat, T. Fractional analysis of co-existence of some types of chaos synchronization. *Chaos Solitons Fractals* **2017**, *105*, 215–223. [CrossRef]

36. Ouannas, A.; Wang, X.; Pham, V.T.; Grassi, G.; Ziar, T. Coexistence of identical synchronization, antiphase synchronization and inverse full state hybrid projective synchronization in different dimensional fractional-order chaotic systems. *Adv. Differ. Equ.* **2018**, *2018*, 35. [CrossRef]

37. Ouannas, A.; Wang, X.; Pham, V.T.; Ziar, T. Dynamic analysis of complex synchronization scheme between integer-order and fractional-order chaotic systems with different dimensions. *Complexity* **2017**, *2017*, 1–12. [CrossRef]

38. Ouannas, A.; Zehrour, O.; Laadjal, Z. Nonlinear methods to control synchronization between fractional-order and integer-order chaotic systems. *Nonlinear Stud.* **2018**, *25*, 1–13.

39. Ouannas, A.; Azar, A.T.; Abu-Saris, R. A new type of hybrid synchronization between arbitrary hyperchaotic maps. *Int. J. Mach. Learn. Cyb.* **2017**, *8*, 1–8. [CrossRef]

40. Ouannas, A. Co-existence of various types of synchronization between hyperchaotic maps. *Nonlinear Dyn. Syst. Theory* **2016**, *16*, 312–321.

41. Ouannas, A.; Grassi, G. A new approach to study co-existence of some synchronization types between chaotic maps with different dimensions. *Nonlinear Dyn.* **2016**, *86*, 1319–1328. [CrossRef]

42. Cermak, J.; Gyori, I.; Nechvatal, L. On explicit stability condition for a linear fractional difference system. *Fract. Calc. Appl. Anal.* **2015**, *18*, 651–672. [CrossRef]

43. Eckmann, J.P.; Ruelle, D. Ergodic theory of chaos and strange attractors. *Rev. Mod. Phys.* **1985**, *57*, 617. [CrossRef]

44. Pincus, S.M. Approximate entropy as a measure of system complexity. *Proc. Natl. Acad. Sci. USA* **1991**, *88*, 2297–2301. [CrossRef] [PubMed]

45. Pincus, S. Approximate entropy (ApEn) as a complexity measure. *Chaos Interdiscipl. J. Nonlinear Sci.* **1995**, *5*, 110–117. [CrossRef] [PubMed]

46. Xu, G.H.; Shekofteh, Y.; Akgal, A.; Li, C.B.; Panahi, S.A. New chaotic system with a self-excited attractor: Entropy measurement, signal encryption, and parameter estimation. *Entropy* **2018**, *20*, 86. [CrossRef]

47. Wang, C.; Ding, Q. A new two-dimensional map with hidden attractors. *Entropy* **2018**, *20*, 322. [CrossRef]

48. Abu-Saris, R.; Al-Mdallal, Q. On the asymptotic stability of linear system of fractional order difference equations. *Fract. Calc. Appl. Anal.* **2013**, *16*, 613–629. [CrossRef]

49. Mozyrska, D.; Wyrwas, M. The Z–transform method and Delta type fractional difference operators. *Discrete Dyn. Nat. Soc.* **2013**, *2013*, 852734. [CrossRef]